Controlling the Superconducting Transition by Rotation of an Inversion Symmetry-Breaking Axis

Lina G. Johnsen,* Kristian Svalland, and Jacob Linder
Center for Quantum Spintronics, Department of Physics, Norwegian University of Science and Technology, NO-7491 Trondheim, Norway

(Received 3 September 2019; revised 28 April 2020; accepted 10 August 2020; published 3 September 2020)

We consider a hybrid structure where a material with Rashba-like spin-orbit coupling is proximity coupled to a conventional superconductor. We find that the superconducting critical temperature T_c can be tuned by rotating the vector $\boldsymbol{n}$ characterizing the axis of broken inversion symmetry. This is explained by a leakage of s-wave singlet Cooper pairs out of the superconducting region, and by conversion of s-wave singlets into other types of correlations, among these s-wave odd-frequency pairs robust to impurity scattering. These results demonstrate a conceptually different way of tuning T_c compared to the previously studied variation of T_c in magnetic hybrids.

DOI: 10.1103/PhysRevLett.125.107002

Introduction.—Over the last years, research on combining superconducting and magnetic materials has shown that the physical properties of the resulting hybrid structure may be drastically altered compared to those of the individual materials [1–3]. In a conventional superconductor (S), electrons combine into s-wave singlet Cooper pairs [4]. A decrease in the s-wave singlet amplitude leads to a loss of superconducting condensation energy, and thus also a suppression of the superconducting critical temperature T_c. Such a decrease can be obtained by leakage of Cooper pairs into a nonsuperconducting material in proximity to the superconductor, and by conversion of s-wave singlets into different singlet and triplet Cooper pairs. For the latter to happen, the nonsuperconducting material must introduce additional symmetry breaking. This is the case in superconductor-ferromagnet hybrids where the spin splitting of the energy bands of the homogeneous ferromagnetic material (F) leads to creation of opposite-spin triplets [2,3,5].

A single, homogeneous ferromagnet cannot alone cause variation in the s-wave singlet amplitude under rotations of the magnetization $\boldsymbol{m}$. However, experiments [6–10] have demonstrated that the critical temperature of $F/S/F$ and $S/F/F$ structures can be modulated by changing the relative orientation of the magnetization of the ferromagnets. The misalignment opens all three triplet channels, leading to a stronger decrease in the superconducting condensation energy associated with the singlet amplitude. Recent work [11–15] has shown that the rotational invariance of the S/F structure can also be broken by adding thin heavy normal-metal layers that boost the interfacial Rashba spin-orbit coupling. Spin-orbit coupling (SOC) introduces inversion symmetry breaking perpendicular to an axis, here characterized by the vector $\boldsymbol{n}$.

While ferromagnetism only leads to spin splitting of the energy bands of spin-up and spin-down electrons, Rashba SOC is in addition odd under inversion of the momentum component perpendicular to $\boldsymbol{n}$. This raises an interesting question. While the proximity effect and accompanying change in T_c in a S/F bilayer is invariant under rotations of $\boldsymbol{m}$, is it possible that T_c in a S/SOC bilayer is *not* invariant under rotations of $\boldsymbol{n}$ (see Fig. 1)?

Motivated by this, we explore the possibility of T_c modulation under reorientations of the inversion symmetry-breaking vector $\boldsymbol{n}$ in a bilayer consisting of a conventional superconductor and a material with Rashba-like SOC in the bulk. We also include interfacial Rashba SOC with an inversion symmetry-breaking vector $\boldsymbol{n}_{\text{int}}$ perpendicular to the interface. This simple model illustrates the concept of tuning T_c via rotation of $\boldsymbol{n}$.

When the bulk SOC is stronger than the interfacial contribution, we discover a suppression of T_c when rotating $\boldsymbol{n}$ from an out-of-plane (OOP) to an in-plane (IP) orientation. This effect is enhanced by increasing the interfacial SOC, provided that $\boldsymbol{n}||\boldsymbol{n}_{\text{int}}$ when $\boldsymbol{n}$ is OOP. The difference in T_c for IP and OOP orientations of $\boldsymbol{n}$ can at least partly be accounted for by the absence of s-wave odd-frequency triplets for an OOP orientation of $\boldsymbol{n}$. Since s-wave triplets are robust with respect to impurity scattering, we expect our prediction of an IP suppression of T_c to be observable

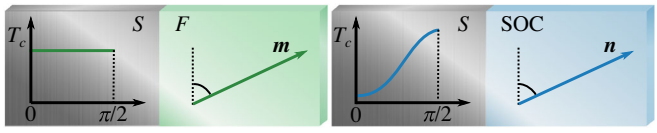

FIG. 1. In a S/F bilayer (left), T_c is invariant under a rotation of $\boldsymbol{m}$. In a S/SOC bilayer (right), the inversion symmetry perpendicular to $\boldsymbol{n}$ is broken. This opens up the possibility for a variation in T_c under a rotation of $\boldsymbol{n}$.

not only in the ballistic limit covered by our theoretical framework, but also in the diffusive limit. When interfacial SOC dominates, the T_c modulation changes qualitatively. The critical temperature is instead suppressed for antiparallel compared to parallel $\boldsymbol{n}$ and $\boldsymbol{n}_{\mathrm{int}}$. This is explained by a reduced leakage of s-wave singlets into the nonsuperconducting region when the total SOC magnitude is increased. Moreover, we demonstrate a variation in T_c even when $\boldsymbol{n}$ is varied solely in the plane of the SOC layer.

The lattice Bogoliubov–de Gennes framework.—We consider a 3D cubic S/SOC lattice structure of size $N_x \times N_y \times N_z$ with interface normal along the x axis. We assume periodic boundary conditions along the y and z axes. The inversion symmetry breaking in the nonsuperconducting layer is accounted for by the existence of a Rashba SOC term in the Hamiltonian, with a constant magnitude λ. In addition, we include a perpendicular Rashba contribution with $\boldsymbol{n}_{\mathrm{int}} = \boldsymbol{x}$ and magnitude λ_{int} at the atomic layer closest to the interface. Our Hamiltonian thus accounts for both a Rashba-like SOC field in the bulk of the nonsuperconducting material, and interfacial Rashba SOC. We use the ballistic-limit tight-binding Bogoliubov–de Gennes framework, following a similar approach to that in Refs. [15–17]. Our Hamiltonian is given by

$$\begin{aligned} H = & -t\sum_{\langle \boldsymbol{i},\boldsymbol{j}\rangle,\sigma} c^{\dagger}_{\boldsymbol{i},\sigma} c_{\boldsymbol{j},\sigma} - \sum_{\boldsymbol{i},\sigma} \mu_{\boldsymbol{i}} c^{\dagger}_{\boldsymbol{i},\sigma} c_{\boldsymbol{i},\sigma} \\ & - \sum_{\boldsymbol{i}} U_{\boldsymbol{i}} n_{\boldsymbol{i},\uparrow} n_{\boldsymbol{i},\downarrow} - \frac{i}{2} \sum_{\langle \boldsymbol{i}\boldsymbol{j}\rangle,\alpha,\beta} c^{\dagger}_{\boldsymbol{i},\alpha} (\lambda \boldsymbol{n} + \lambda_{\mathrm{int}} \boldsymbol{n}_{\mathrm{int}}) \\ & \cdot \left\{ \boldsymbol{\sigma} \times \left[\frac{1}{2}(1+\zeta)(\boldsymbol{d}_{\boldsymbol{i}\boldsymbol{j}})_x + (\boldsymbol{d}_{\boldsymbol{i}\boldsymbol{j}})_{||} \right] \right\}_{\alpha,\beta} c_{\boldsymbol{j},\beta}. \end{aligned} \tag{1}$$

Above, t is the hopping integral, $\mu_{\boldsymbol{i}}$ is the chemical potential at lattice site $\boldsymbol{i}$, $U_{\boldsymbol{i}} > 0$ is the attractive on-site interaction giving rise to superconductivity, $\boldsymbol{\sigma}$ is the vector of Pauli matrices, $\boldsymbol{d}_{\boldsymbol{i}\boldsymbol{j}}$ is the vector from site $\boldsymbol{i}$ to site $\boldsymbol{j}$, and $(\boldsymbol{d}_{\boldsymbol{i}\boldsymbol{j}})_x$ and $(\boldsymbol{d}_{\boldsymbol{i}\boldsymbol{j}})_{||}$ are its projections onto the x axis and yz plane, respectively. If site $\boldsymbol{i}$ and $\boldsymbol{j}$ are both inside the SOC layer, $\zeta = 1$. Otherwise, $\zeta = 0$. $c^{\dagger}_{\boldsymbol{i},\sigma}$ and $c_{\boldsymbol{i},\sigma}$ are the second quantization electron creation and annihilation operators at site $\boldsymbol{i}$ with spin σ, and $n_{\boldsymbol{i},\sigma} \equiv c^{\dagger}_{\boldsymbol{i},\sigma} c_{\boldsymbol{i},\sigma}$ is the number operator. The Rashba term [18] has been symmetrized in order to allow for IP components of $\boldsymbol{n}$ while ensuring a Hermitian Hamiltonian. The superconducting term is treated by a mean-field approach, assuming $c_{\boldsymbol{i},\uparrow} c_{\boldsymbol{i},\downarrow} = \langle c_{\boldsymbol{i},\uparrow} c_{\boldsymbol{i},\downarrow}\rangle + \delta$ and neglecting terms of second order in the fluctuations δ. The terms of the Hamiltonian are only nonzero in their respective regions.

We diagonalize the Hamiltonian numerically and compute the physical quantities of interest as outlined in the Supplemental Material [19]. The superconducting gap $\Delta_{\boldsymbol{i}} \equiv U_{\boldsymbol{i}} \langle c_{\boldsymbol{i},\uparrow} c_{\boldsymbol{i},\downarrow}\rangle$ is treated iteratively. We calculate T_c by a binomial search [20] where we for each of the N_T temperatures considered decide whether the gap increases toward a superconducting state or decreases toward a normal state from an initial guess much smaller than the zero-temperature gap. In this way, we do not calculate the exact value for the gap, and we can thus get high accuracy in T_c for a low number of iterations N_Δ.

In order to confirm that the modulation of T_c is caused by conversion of s-wave even-frequency singlets into other singlet and triplet correlations, we consider the even-frequency s-wave singlet amplitude $S_{s,\boldsymbol{i}} \equiv \langle c_{\boldsymbol{i},\uparrow} c_{\boldsymbol{i},\downarrow}\rangle - \langle c_{\boldsymbol{i},\downarrow} c_{\boldsymbol{i},\uparrow}\rangle$. As a measure of the total s-wave singlet amplitude of the superconductor, we introduce the quantity $\mathcal{S} \equiv (1/N_{x,S}) \sum_i |S_{s,i}|$, where the sum is taken over the superconducting region only. We also define the opposite- and equal-spin odd-frequency s-wave triplet amplitudes $S_{0,\boldsymbol{i}}(\tau) \equiv \langle c_{\boldsymbol{i},\uparrow}(\tau) c_{\boldsymbol{i},\downarrow}(0)\rangle + \langle c_{\boldsymbol{i},\downarrow}(\tau) c_{\boldsymbol{i},\uparrow}(0)\rangle$ and $S_{\sigma,\boldsymbol{i}}(\tau) \equiv \langle c_{\boldsymbol{i},\sigma}(\tau) c_{\boldsymbol{i},\sigma}(0)\rangle$ [17], where the time-dependent electron annihilation operator is given by $c_{\boldsymbol{i},\sigma}(\tau) \equiv e^{iH\tau} c_{\boldsymbol{i},\sigma} e^{-iH\tau}$ [21]. The s-wave triplet amplitude is of particular interest as it is the only triplet amplitude robust to impurity scattering. Other superconducting correlations, such as p-wave and d-wave correlations, also appear due to the presence of SOC, as will be discussed later in this work.

The superconducting critical temperature.—By following the above approach, we plot the critical temperature and the total s-wave singlet amplitude in Fig. 2. To ensure that the effect is robust, we use two different parameter sets. The parameters are given in the figure caption. All length scales are scaled by the lattice constant a, the SOC magnitudes are scaled by ta, and the remaining energy scales are scaled by t. For $t \sim 1$ eV and $a \sim 5$ Å, the order of magnitude of λ is 10^{-10} eVm, which corresponds well to Rashba parameters found in several materials [22]. In order to make the system computationally manageable, the lattice size and coherence length $\xi \propto \Delta^{-1}$ must be scaled down, leading to an overestimation of Δ and thus T_c. The results in Fig. 2 must therefore be seen mainly as qualitative.

For both sets of parameters, we see a qualitatively similar behavior for rotations of $\boldsymbol{n}$ in the xz plane [see Fig. 2(a) for the first set of parameters]. When $\lambda_{\mathrm{int}} = 0$, we find a suppression of T_c for an IP $\boldsymbol{n}$ compared to an OOP $\boldsymbol{n}$. When $0 < \lambda_{\mathrm{int}} < \lambda$, there are still maxima at the OOP directions $\boldsymbol{n} || \boldsymbol{n}_{\mathrm{int}}$ and $(-\boldsymbol{n}) || \boldsymbol{n}_{\mathrm{int}}$, but when increasing λ_{int} the magnitude of the former increases while the magnitude of the latter decreases. As long as $\boldsymbol{n}$ is parallel to $\boldsymbol{n}_{\mathrm{int}}$ in the OOP configuration, the T_c modulation from IP to OOP is thus enhanced by the additional interface contribution. For $\lambda_{\mathrm{int}} > \lambda$, T_c is maximal for $\boldsymbol{n} || \boldsymbol{n}_{\mathrm{int}}$ and minimal for $(-\boldsymbol{n}) || \boldsymbol{n}_{\mathrm{int}}$. The change in T_c from the parallel to the antiparallel configuration increases with an increasing λ_{int}. The results presented here only depend on the relative orientations of $\boldsymbol{n}$ and $\boldsymbol{n}_{\mathrm{int}}$, and are independent of whether $\boldsymbol{n}_{\mathrm{int}}$ is directed out of or into the nonsuperconducting material. Notice that in all cases, nonzero SOC increases T_c compared to when $\lambda = \lambda_{\mathrm{int}} = 0$. This is explained by a

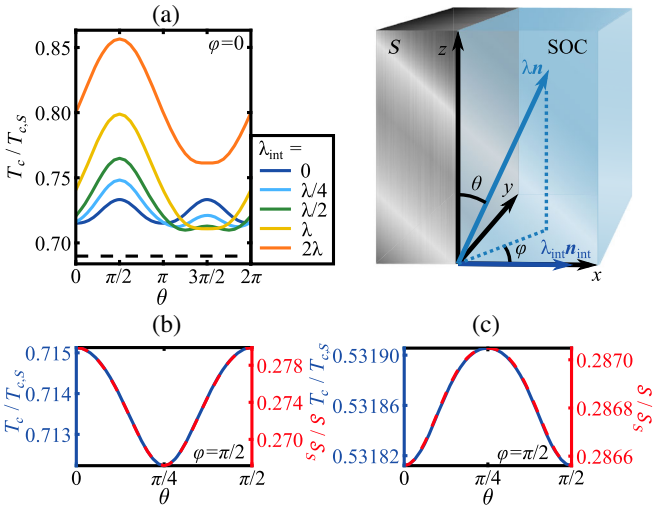

FIG. 2. The T_c modulation under rotation of $\boldsymbol{n}$ between IP and OOP orientations (a) is qualitatively different for $\lambda_{\rm int} < \lambda$ and $\lambda_{\rm int} > \lambda$. The dashed line marks T_c for $\lambda = \lambda_{\rm int} = 0$. Depending on the material parameters, T_c can have either its IP maxima (b) or minima (c) along the cubic axes. Notice the strong correlation between T_c and the total s-wave singlet amplitude at $T = T_c^-$. Above, $T_{c,S}$ and $\mathcal{S}_S$ corresponds to when the superconductor is without proximity to the SOC layer. We have used parameters $N_{x,S} = 7$, $N_{x,HM} = 3$, $N_y = N_z = 85$, $\mu_S = 1.9$, $\mu_{HM} = 1.7$, $U = 2.1$, $\lambda = 0.8$, $N_T = 20$, and $N_\Delta = 35$ for panels (a) and (b), and $N_{x,S} = 5$, $N_{x,HM} = 2$, $N_y = N_z = 100$, $\mu_S = 1.9$, $\mu_{HM} = 1.7$, $U = 1.9$, $\lambda = 0.2$, $N_T = 25$, and $N_\Delta = 40$ for panel (c), corresponding to coherence lengths $\xi = 4$ and $\xi = 7$, respectively. In panels (b) and (c), $\lambda_{\rm int} = 0$.

decreased leakage of conventional singlets into the nonsuperconducting region.

From panels (b) and (c), we see that there is also an IP variation in T_c, that may give the strongest in-plane suppression either when $\boldsymbol{n}$ is oriented at a $\pi/4$ angle with respect to the cubic axes, or when $\boldsymbol{n}$ is oriented along the cubic axes. As we find a similar variation in the normal-state free energy, which only depends on the eigenenergy spectrum of the system, this varying modulation of the IP component of T_c is likely to be caused by band-structure effects due to the crystal structure of the cubic lattice. In order to demonstrate the IP modulation, the interfacial SOC should preferably be as small as possible.

To demonstrate that the T_c modulation can be attributed to the variation of the s-wave singlet amplitude in the superconducting region, we plot the total s-wave singlet amplitude as a function of the IP angle of $\boldsymbol{n}$ [panels (b) and (c)]. As expected, it is of a similar form as the variation in T_c. The slight deviation between T_c and $\mathcal{S}$ is caused by $\mathcal{S}$ being calculated at a temperature T_c^- slightly below T_c. We have verified that the variation in $\mathcal{S}$ and T_c is similar also for panel (a).

The variation in the s-wave singlet amplitude inside the superconducting region is caused by a reduced leakage of s-wave singlets out of the superconducting region, and conversion of s-wave singlets into other singlet and triplet correlations. When $\lambda_{\rm int}$ is nonzero, the length of $\lambda\boldsymbol{n} + \lambda_{\rm int}\boldsymbol{n}_{\rm int}$ changes under rotations of $\boldsymbol{n}$, leading to an effective change in the magnitude of the SOC. Increased SOC causes an increase in the Fermi vector mismatch [23], due to a change in the Fermi surface in the nonsuperconducting material. Since the overlap between the Fermi surfaces of the two materials decreases, there is an increase in the normal reflection at the interface, as our analytical results verify. For large $\lambda_{\rm int}$, the T_c modulation is dominated by variation in the Fermi vector mismatch. If we further investigate the triplet amplitudes present for different orientations of $\boldsymbol{n}$, we find that the s-wave odd-frequency triplet amplitude is absent for $\boldsymbol{n} = \boldsymbol{x}$, i.e., when $\boldsymbol{n}$ has no IP component. For all other orientations of $\boldsymbol{n}$, the s-wave odd-frequency anomalous triplet amplitude is nonzero. This suggests that the OOP to IP change in T_c is at least partly caused by the increase in the s-wave triplet amplitude from zero when $\boldsymbol{n}$ points OOP to an increasing finite value as the IP component of $\boldsymbol{n}$ increases. When $\lambda_{\rm int}$ is small, so that the length of $\lambda\boldsymbol{n} + \lambda_{\rm int}\boldsymbol{n}_{\rm int}$ is approximately constant, we may therefore expect an IP suppression of T_c not only in the ballistic-limit materials covered by our theoretical framework, but also in diffusive materials. Below, we perform analytical calculations which prove that odd-frequency pairing is absent when $\boldsymbol{n}$ points OOP.

The continuum Bogoliubov–de Gennes framework.—In order to explain the absence of s-wave odd-frequency triplets when $\boldsymbol{n}$ is OOP, we consider two 2D continuum systems that can be treated analytically within the Bogoliubov–de Gennes framework [24–31]: a SOC/S bilayer with an OOP $\boldsymbol{n} = \boldsymbol{x}$, and a F/S bilayer with magnetization $\boldsymbol{m} \| \boldsymbol{z}$. We use conventions similar to those in Refs. [30,31]. Our systems are located in the xy plane, with interface normal along $\boldsymbol{x}$ and the interface at $x = 0$.

We find the scattering wave functions $\Psi_n(x_1)$ and $\tilde{\Psi}_m(x_2)$ that we will use to construct the Green's functions in the system from the time-independent Schrödinger equations [30–32]

$$\begin{aligned} H(p_y)\Psi_n(x_1) &= (\omega + i\delta)\Psi_n(x_1), \\ H^*(p_y)\tilde{\Psi}_m(x_2) &= (\omega + i\delta)\tilde{\Psi}_m(x_2), \end{aligned} \tag{2}$$

respectively, where

$$\begin{aligned} H(p_y) = {} & (-\partial_x^2/\eta + p_y^2/\eta - \mu)\hat{\tau}_3\hat{\sigma}_0 \\ & + \Delta i\hat{\tau}^+\hat{\sigma}_y - \Delta^* i\hat{\tau}^-\hat{\sigma}_y + h_x\hat{\tau}_3\hat{\sigma}_x + h_y\hat{\tau}_0\hat{\sigma}_y + h_z\hat{\tau}_3\hat{\sigma}_z \\ & - \lambda(n_x p_y + n_y i\partial_x)\hat{\tau}_0\hat{\sigma}_z + i\lambda n_z\partial_x\hat{\tau}_3\hat{\sigma}_y + \lambda n_z p_y\hat{\tau}_0\hat{\sigma}_x. \end{aligned} \tag{3}$$

Above, $\delta > 0$ is real and infinitesimal, $\eta \equiv 2m/\hbar^2$, p_y is the momentum in the y direction, and $\boldsymbol{h} = (h_x, h_y, h_z)$ is the magnetic exchange field. The terms are only nonzero in their respective regions. The four components of the

scattering wave functions correspond to spin-up and spin-down electrons, and spin-up and spin-down holes, respectively. The spins are defined with respect to the z axis. The indices n and m refer to the eight possible wave functions describing scattering of quasiparticles incoming from the left and right. In the continuum model, the symmetrization of the Rashba term enters through the boundary conditions of the wave functions at $x = 0$ rather than through the Hamiltonian [33]. From the scattering wave functions, we construct the retarded Green's function in Nambu $\otimes$ spin space for $x_1 > x_2$ and $x_1 < x_2$, and apply boundary conditions at $x_1 = x_2$.

The even-(odd-)frequency singlet and triplet retarded anomalous Green's functions can be written in terms of the center of mass coordinate $X \equiv (x_1 + x_2)/2$ and the relative coordinate $x \equiv x_1 - x_2$ as [30,31]

$$\begin{aligned} F_0^{r,E(O)}(X,x,p_y;\omega) &= [F_0^r(X,x,p_y;\omega) \underset{(-)}{+} F_0^r(X,-x,-p_y;\omega)]/2, \\ F_i^{r,E(O)}(X,x,p_y;\omega) &= [F_i^r(X,x,p_y;\omega) \underset{(+)}{-} F_i^r(X,-x,-p_y;\omega)]/2, \end{aligned} \tag{4}$$

where $i = \{1,2,3\}$, and

$$\begin{aligned} F_0^r(X,x,p_y;\omega) &= [F_{\uparrow\downarrow}^r(X,x,p_y;\omega) - F_{\downarrow\uparrow}^r(X,x,p_y;\omega)]/2, \\ F_1^r(X,x,p_y;\omega) &= F_{\uparrow\uparrow}^r(X,x,p_y;\omega), \\ F_2^r(X,x,p_y;\omega) &= F_{\downarrow\downarrow}^r(X,x,p_y;\omega), \\ F_3^r(X,x,p_y;\omega) &= [F_{\uparrow\downarrow}^r(X,x,p_y;\omega) + F_{\downarrow\uparrow}^r(X,x,p_y;\omega)]/2 \end{aligned} \tag{5}$$

represents the singlet amplitude, the equal-spin triplet amplitudes ($i = 1, 2$), and the opposite-spin triplet amplitude ($i = 3$), respectively. The retarded anomalous Green's functions $F_{\sigma\sigma'}^r(X,x,p_y;\omega)$ are anomalous elements of the retarded Green's function in Nambu $\otimes$ spin space. Odd (even) frequency refers to the sum of the retarded and advanced Green's functions being odd (even) under inversion of relative time, or equivalently under inversion of the sign of ω.

The analytical expressions obtained for the even- and odd-frequency singlet and triplet retarded anomalous Green's functions are given in the Supplemental Material [19]. Their spatial symmetries are determined by their parities under inversion of x and p_y. Although the s-wave and $d_{x^2-y^2}$-wave triplets have the same parities along the x and y axis, the presence of the s-wave triplet is proven by a nonzero result when integrating over all spatial coordinates.

Singlet and triplet amplitudes.—For the 2D SOC/S structure with $\boldsymbol{n} = \boldsymbol{x}$, we find that s- and p_x-wave singlets, and p_y- and d_{xy}-wave opposite-spin triplets are present.

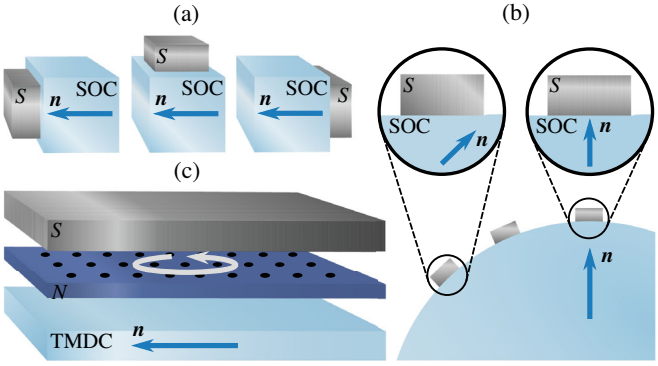

FIG. 3. For the experimental observation of the IP to OOP T_c modulation, we suggest growing the superconductor on (a) different surfaces of a noncentrosymmetric material or (b) on a curved noncentrosymmetric material. For observing IP variations, we suggest (c) growing a normal metal with a cubic lattice structure at different angles compared to a TMDC with IP inversion symmetry breaking, and then growing the superconductor on top. The N/TMDC bilayer effectively enables a rotation of $\boldsymbol{n}$ compared to the lattice.

At the first glance, it might seem strange that the odd-frequency s-wave triplet amplitude is zero, when it is nonzero for a 2D F/S structure with magnetization along the z axis. Although the Hamiltonians of these systems are of a similar form, they allow for the existence of different triplet amplitudes. The crucial difference leading to a generation of p_y- and d_{xy}-wave triplets in the SOC/S system rather than s- and p_x-wave triplets as in the F/S system, is the momentum dependence of the Rashba term.

We have also investigated a 2D SOC/S structure for an IP orientation $\boldsymbol{n} = \boldsymbol{z}$ numerically and find additional equal-spin triplets with an odd-frequency symmetry. For a 3D SOC/S system with $\boldsymbol{n}$ OOP, the Rashba term depends on the momentum both along the y and z axes. Similarly as in 2D, we expect this to allow for triplets that are odd under inversion of p_y and p_z. This is ultimately the reason for the absence of s-wave triplets.

Experimental realization.—We finally comment on the possibilities of an experimental realization of the predicted T_c variation upon redirecting $\boldsymbol{n}$. We suggest cleaving a noncentrosymmetric metal, such as BiPd [34–36], in different directions and growing a superconductor (with a higher T_c) on the surface, see Fig. 3(a). This requires a material that can be cleaved along at least two axes. Alternatively, one could deposit superconductors on the surface of a curved noncentrosymmetric material with a long edge (several mm), see Fig. 3(b) [37]. In both scenarios, different samples would have their inversion symmetry-breaking axis in different directions, corresponding to a systematic rotation of $\boldsymbol{n}$ from IP to OOP. We underline that although $\boldsymbol{n}$ rotates along with the lattice in the nonsuperconducting region, the difference in T_c as $\boldsymbol{n}$ changes from IP to OOP is robust. The reason is that the corresponding change in the proximity effect

exists even in our continuum model without the underlying lattice.

In order to observe IP variations, we suggest growing a normal metal (N) with a cubic lattice structure at different angles compared to a transition metal dichalcogenide (TMDC) with IP inversion symmetry breaking [38], see Fig. 3(c). This corresponds to an effective IP rotation of $\boldsymbol{n}$ compared to the lattice. The superconductor is grown on top of the normal metal, which should be a light element with as little interfacial SOC as possible. The ideal scenario, albeit challenging, would be to induce an *in situ* rotation of $\boldsymbol{n}$ in the nonsuperconducting region via electric gating in different directions, that induces an inversion-symmetry-breaking field. However, since $\boldsymbol{n}$ is rotated inside the noncentrosymmetric material, λ may in principle vary. This is not the case for our previous suggestions, since we do not rotate $\boldsymbol{n}$ inside the noncentrosymmetric material, but instead change the position of the superconductor.

Concluding, we have shown that the superconducting transition temperature T_c can be altered by rotating the inversion symmetry-breaking axis $\boldsymbol{n}$ in a proximate material, providing a conceptually different way of controlling T_c compared to previous studies. Moreover, we have shown that when in addition an interfacial spin-orbit coupling perpendicular to the interface is present and substantial, the behavior of T_c as $\boldsymbol{n}$ is varied can change qualitatively.

The authors would like to thank J. A. Ouassou, and J. W. Wells for helpful discussions. This work was supported by the Research Council of Norway through its Centres of Excellence funding scheme Grant No. 262633 QuSpin.

*Corresponding author.
lina.g.johnsen@ntnu.no

[1] J. Linder and J. W. A. Robinson, Superconducting spintronics, Nat. Phys. **11**, 307 (2015).
[2] M. Eschrig, Spin-polarized supercurrents for spintronics: a review of current progress, Phys. Today **64**, No. 1, 43 (2011).
[3] M. Eschrig, Spin-polarized supercurrents for spintronics: a review of current progress, Rep. Prog. Phys. **78**, 104501 (2015).
[4] J. Bardeen, L. N. Cooper, and J. R. Schrieffer, Theory of superconductivity, Phys. Rev. **108**, 1175 (1957).
[5] J. Linder and A. V. Balatsky, Odd-frequency superconductivity, Rev. Mod. Phys. **91**, 045005 (2019).
[6] J. Y. Gu, C. Y. You, J. S. Jiang, J. Pearson, Y. B. Bazaliy, and S. D. Bader, Magnetization-Orientation Dependence of the Superconducting Transition Temperature in the Ferromagnet-Superconductor-Ferromagnet System: CuNi/Nb/CuNi, Phys. Rev. Lett. **89**, 267001 (2002).
[7] I. C. Moraru, W. P. Pratt, and N. O. Birge, Magnetization-Dependent T_c Shift in Ferromagnet/Superconductor/Ferromagnet Trilayers with a Strong Ferromagnet, Phys. Rev. Lett. **96**, 037004 (2006).
[8] P. V. Leksin, N. N. Garif'yanov, I. A. Garifullin, Y. V. Fominov, J. Schumann, Y. Krupskaya, V. Kataev, O. G. Schmidt, and B. Büchner, Evidence for Triplet Superconductivity in a Superconductor-Ferromagnet Spin Valve, Phys. Rev. Lett. **109**, 057005 (2012).
[9] N. Banerjee, C. B. Smiet, R. G. J. Smits, A. Ozaeta, F. S. Bergeret, M. G. Blamire, and J. W. A. Robinson, Evidence for spin selectivity of triplet pairs in superconducting spin valves, Nat. Commun. **5**, 3048 (2014).
[10] X. L. Wang, A. Di Bernardo, N. Banerjee, A. Wells, F. S. Bergeret, M. G. Blamire, and J. W. A. Robinson, Giant triplet proximity effect in superconducting pseudo spin valves with engineered anisotropy, Phys. Rev. B **89**, 140508(R) (2014).
[11] S. H. Jacobsen, J. A. Ouassou, and J. Linder, Critical temperature and tunneling spectroscopy of superconductor-ferromagnet hybrids with intrinsic Rashba-Dresselhaus spin-orbit coupling, Phys. Rev. B **92**, 024510 (2015).
[12] J. A. Ouassou, A. D. Bernardo, J. W. A. Robinson, and J. Linder, Electric control of superconducting transition through a spin-orbit coupled interface, Sci. Rep. **6**, 29312 (2016).
[13] H. T. Simensen and J. Linder, Tunable superconducting critical temperature in ballistic hybrid structures with strong spin-orbit coupling, Phys. Rev. B **97**, 054518 (2018).
[14] N. Banerjee, J. A. Ouassou, Y. Zhu, N. A. Stelmashenko, J. Linder, and M. G. Blamire, Controlling the superconducting transition by spin-orbit coupling, Phys. Rev. B **97**, 184521 (2018).
[15] L. G. Johnsen, N. Banerjee, and J. Linder, Magnetization reorientation due to the superconducting transition in heavy-metal heterostructures, Phys. Rev. B **99**, 134516 (2019).
[16] D. Terrade, Proximity effects and Josephson currents in ferromagnet-spin-triplet superconductors junctions, Ph.D. thesis, Max-Planck-Institut für Festkörperforschung, Universität Stuttgart, 2015.
[17] J. Linder, M. Amundsen, and V. Risinggård, Intrinsic superspin Hall current, Phys. Rev. B **96**, 094512 (2017).
[18] Y. A. Bychkov and E. I. Rashba, Oscillatory effects and the magnetic susceptibility of carriers in inversion layers, J. Phys. C **17**, 6039 (1984).
[19] See Supplemental Material at http://link.aps.org/supplemental/10.1103/PhysRevLett.125.107002 for a further description of the lattice Bogoliubov-de Gennes framework, where we derive the symmetrized Rashba contribution to the Hamiltonian, diagonalize the Hamiltonian, and calculate the relevant physical quantities such as the superconducting critical temperature and the total s-wave singlet amplitude, and for a further description of the continuum Bogoliubov-de Gennes framework, where we give explicit expressions for the wave functions, and for the even- and odd-frequency singlet and triplet retarded anomalous Green's functions as well as tables of their symmetries.
[20] J. A. Ouassou, Density of states and critical temperature in superconductor/ferromagnet structures with spin-orbit coupling, Master's thesis, Norwegian University of Science and Technology, 2015.
[21] A. L. Fetter and J. D. Walexka, *Quantum Theory of Many-Particle Systems* (Dover Publications Inc., Mineola, New York, 2003).

[22] A. Manchon, H. C. Koo, J. Nitta, S. M. Frolov, and R. A. Duine, New perspectives for Rashba spin–orbit coupling, Nat. Mater. **14**, 871 (2015).
[23] Y. Tanaka and M. Tsukada, Theory of superconducting proximity effect in a three-dimensional system in the clean limit, Phys. Rev. B **42**, 2066 (1990).
[24] W. L. McMillan, Theory of superconductor–normal-metal interfaces, Phys. Rev. **175**, 559 (1968).
[25] C. Ishii, Josephson currents through junctions with normal metal barriers, Prog. Theor. Phys. **44**, 1525 (1970).
[26] A. Furusaki and M. Tsukada, Dc Josephson effect and Andreev reflection, Solid State Commun. **78**, 299 (1991).
[27] S. Kashiwaya and Y. Tanaka, Tunnelling effects on surface bound states in unconventional superconductors, Rep. Prog. Phys. **63**, 1641 (2000).
[28] R. T. W. Koperdraad, R. E. S. Otadoy, M. Blaauboer, and A. Lodder, Multiple-scattering theory for clean superconducting layered structures, J. Phys. Condens. Matter **13**, 8707 (2001).
[29] B. Lu and Y. Tanaka, Study on Green's function on topological insulator surface, Phil. Trans. R. Soc. A **376**, 20150246 (2018).
[30] J. Cayao and A. M. Black-Schaffer, Odd-frequency superconducting pairing and subgap density of states at the edge of a two-dimensional topological insulator without magnetism, Phys. Rev. B **96**, 155426 (2017).
[31] J. Cayao and A. M. Black-Schaffer, Odd-frequency superconducting pairing in junctions with Rashba spin-orbit coupling, Phys. Rev. B **98**, 075425 (2018).
[32] G. E. Blonder, M. Tinkham, and T. M. Klapwijk, Transition from metallic to tunneling regimes in superconducting microconstrictions: Excess current, charge imbalance, and supercurrent conversion, Phys. Rev. B **25**, 4515 (1982).
[33] C. R. Reeg and D. L. Maslov, Proximity-induced triplet superconductivity in Rashba materials, Phys. Rev. B **92**, 134512 (2015).
[34] N. N. Zhuravlev, Structure of superconductors. X: Thermal, microscopic and X-ray investigation of the bismuth-palladium system, Sov. Phys. JETP **5**, 1064 (1957), http://www.jetp.ac.ru/cgi-bin/dn/e_005_06_1064.pdf.
[35] Y. Bhatt and K. Schubert, Kristallstruktur von PdBi.r, J. Less-Common Met. **64**, P17 (1979).
[36] Z. Sun, M. Enayat, A. Maldonado, C. Lithgow, E. Yelland, D. C. Peets, A. Yaresko, A. P. Schnyder, and P. Wahl, Dirac surface states and nature of superconductivity in Noncentrosymmetric BiPd, Nat. Commun. **6**, 6633 (2015).
[37] J. E. Ortega, M. Corso, Z. M. Abd-el-Fattah, E. A. Goiri, and F. Schiller, Interplay between structure and electronic states in step arrays explored with curved surfaces, Phys. Rev. B **83**, 085411 (2011).
[38] M. A. U. Absor, I. Santoso, Harsojo, K. Abrasha, H. Kotaka, F. Ishii, and M. Saito, Polarity tuning of spin-orbit-induced spin splitting in two-dimensional transition metal dichalcogenides, J. Appl. Phys. **122**, 153905 (2017).